Sensitive Detection of Phosphorus Deficiency in Plants Using Chlorophyll *a* Fluorescence[1]

Jens Frydenvang[2]*, Marie van Maarschalkerweerd[2], Andreas Carstensen[2], Simon Mundus, Sidsel Birkelund Schmidt, Pai Rosager Pedas, Kristian Holst Laursen, Jan K. Schjoerring, and Søren Husted*

Department of Plant and Environmental Sciences, Faculty of Science, University of Copenhagen, 1871 Frederiksberg C, Denmark (J.F., M.v.M., A.C., S.M., S.B.S., P.R.P., K.H.L., J.K.S., S.H.); and FOSS Analytical A/S, 3400 Hillerød, Denmark (M.v.M.)

ORCIDIDs:0000-0001-9294-1227(J.F.);0000-0002-2748-3239(M.v.M.);0000-0001-5029-7015(A.C.);0000-0002-2128-8061(S.M.);0000-0002-4193-4454(S.B.S.);0000-0001-6733-7300(P.R.P.);0000-0001-7900-3324(K.H.L.);0000-0002-2852-3298(J.K.S.);0000-0003-2020-1902(S.H.).

Phosphorus (P) is a finite natural resource and an essential plant macronutrient with major impact on crop productivity and global food security. Here, we demonstrate that time-resolved chlorophyll *a* fluorescence is a unique tool to monitor bioactive P in plants and can be used to detect latent P deficiency. When plants suffer from P deficiency, the shape of the time-dependent fluorescence transients is altered distinctively, as the so-called I step gradually straightens and eventually disappears. This effect is shown to be fully reversible, as P resupply leads to a rapid restoration of the I step. The fading I step suggests that the electron transport at photosystem I (PSI) is affected in P-deficient plants. This is corroborated by the observation that differences at the I step in chlorophyll *a* fluorescence transients from healthy and P-deficient plants can be completely eliminated through prior reduction of PSI by far-red illumination. Moreover, it is observed that the barley (*Hordeum vulgare*) mutant *Viridis-zb*^{63}, which is devoid of PSI activity, similarly does not display the I step. Among the essential plant nutrients, the effect of P deficiency is shown to be specific and sufficiently sensitive to enable rapid in situ determination of latent P deficiency across different plant species, thereby providing a unique tool for timely remediation of P deficiency in agriculture.

The world population is estimated to exceed 9 billion people by 2050. This means that agriculture on a global scale has to increase food production by 70% to 100%, and, at the same time, handle the consequences of global climate changes and reduce its environmental footprint (Food and Agriculture Organization of the United Nations, 2009; Godfray et al., 2010; Foley et al., 2011). A major challenge related to this is the supply and use of phosphorus (P) to support future plant production (Cordell et al., 2009; Gilbert, 2009; MacDonald et al., 2011).

P is an essential plant nutrient, which means that plants require P in adequate amounts to fulfill a complete lifecycle. It has been estimated that 30% of the world's agricultural soils are P deficient and need fertilizer addition to ensure yield and quality (MacDonald et al., 2011). However, phosphate rock, the main source of P fertilizers, is a finite natural resource, and the known rock phosphate reserves are estimated to last as little as 50 years in the gloomiest forecasts (Gilbert, 2009; Edixhoven et al., 2013). This makes P a potential strategic natural resource similar to oil, as very few countries control the vast majority of the known reserves (Gilbert, 2009; Elser and Bennett, 2011; Edixhoven et al., 2013). Presently, an immense overuse of P is found in some parts of the world, causing eutrophication of lakes and seas, while P depletion results in severe yield limitations elsewhere (MacDonald et al., 2011; Obersteiner et al., 2013). An essential aspect of solving both of these problems is to increase P use efficiency in agriculture, thus reducing the negative environmental impact of agriculture and helping to ensure a sustainable use of P resources while increasing the worldwide food production (Schröder et al., 2011; Veneklaas et al., 2012).

Here, we present a unique analytical principle based on chlorophyll *a* fluorescence that allows rapid, nondestructive, onsite assessment of plant P status by recording the so-called OJIP transient of a dark-adapted leaf.

When a chlorophyll molecule absorbs light, one of three events will occur: The light may be used to drive photosynthesis, it can be dissipated as heat, or it can be

[1] This work was supported by the Danish Strategic Research Council (NUTRIEFFICIENT; grant no. 10–093498), Foss Analytical A/S, Innovation Fund Denmark, and the University of Copenhagen.

[2] These authors contributed equally to the article.

* Address correspondence to jfr@plen.ku.dk and shu@plen.ku.dk.

The author responsible for distribution of materials integral to the findings presented in this article in accordance with the policy described in the Instructions for Authors (www.plantphysiol.org) is: Søren Husted (shu@plen.ku.dk).

J.F., M.v.M., A.C., and S.H. designed the experiments and performed the fluorescence measurements and multivariate analysis; A.C. and S.M. performed and evaluated field trials; S.B.S., K.H.L., and P.R.P. performed and evaluated fluorescence measurements on plants exposed to nutrient deficiencies other than phosphorus; all authors participated in data interpretation and in writing the final article.

www.plantphysiol.org/cgi/doi/10.1104/pp.15.00823

reemitted as fluorescence. Less than 10% of light absorbed by the plant causes emission of chlorophyll *a* fluorescence (Govindjee, 2004; Stirbet and Govindjee, 2011). When a dark-adapted leaf is exposed to saturating actinic light, the resulting time-dependent fluorescence forms a so-called Kautsky curve (Kautsky and Hirsch, 1931; McAlister and Myers, 1940). Within 300 ms, the fluorescence increases from a minimum level (F_0) to the maximum level. If measured with a sufficiently high time resolution, a polyphasic transient with four distinct steps, designated as O, J, I, and P, is observed. After reaching maximum intensity at the P step, the fluorescence intensity declines until it reaches a steady state within a few minutes (Harbinson and Rosenqvist, 2003; Govindjee, 2004).

The physiological mechanisms underlying the polyphasic OJIP transient are still not clarified, but it is believed that the J and I steps represent dynamic bottlenecks in the photosynthetic electron transport chain. The first rise (2 ms) from O to J is referred to as the photochemical phase due to its dependence on the intensity of the incoming light. This phase is assumed to reflect the reduction of the primary quinone electron acceptor in PSII (Stirbet and Govindjee, 2011). The reduction of the primary quinone electron acceptor results in a decreased electron trapping efficiency and therefore an increase in the dissipation of absorbed light energy by fluorescence and heat. The second part, from J over I to P, is called the thermal phase due to its temperature sensitivity. This phase is much slower than the first, and it is believed that the J-I phase primarily reflects a sequential reduction of the remaining plastoquinone pool of PSII and that the I-P phase reflects the subsequent electron flow through cytochrome b_6f to electron sinks at the PSI acceptor side (Stirbet and Govindjee, 2011). Thus, the OJIP transient resembles a titration of the photochemical quantum yield and reflects the complex electron transport properties of PSII and PSI.

Consistent with their known influence on photosynthesis, deficiencies of essential plant nutrients such as Fe, Cu, Mg, Mn, and S have previously been shown to affect OJIP transients (Kastori et al., 2000; Mallick and Mohn, 2003; Larbi et al., 2004; Husted et al., 2009; Tang et al., 2012; Yang et al., 2012). As a consequence, several attempts have been made to identify nutrient imbalances and disorders using one or several parameters derived from the transients, but apart from Mn (Husted et al., 2009; Schmidt et al., 2013), attempts have not been successful in terms of sensitivity and specificity. This includes P, which previously has been reported to have an effect on OJIP transients, yet the reported effects seem mutually contradictory and nonspecific to P (Ripley et al., 2004; Weng et al., 2008; Jiang et al., 2009; Lin et al., 2009).

Here, we present the unique finding that increasing levels of P deficiency affect the shape of the OJIP transient around the I step at 20 to 50 ms and causes the I step to gradually straighten and disappear. It is demonstrated that this effect is fully reversible and, among the essential plant nutrients, specific for P deficiency using both monocotyledons (barley [*Hordeum vulgare*]) and dicotyledons (tomato [*Solanum lycopersicum*]) plant species. Furthermore, it is shown that it is possible to determine whether a plant is P sufficient or deficient and to quantitatively predict the P concentration in leaf tissue using multivariate analysis of the OJIP transients.

RESULTS

Chlorophyll *a* Fluorescence Measurements Show Characteristic OJIP Transients in P-Deficient Plants

The ability of chlorophyll *a* fluorescence measurements to quantitatively predict the bioactive concentration of P in leaves was investigated in experiments with hydroponically and soil-grown barley and tomato plants. The different growth regimes resulted in plants spanning the full range of foliar P concentrations, from luxury P uptake (>4,000 μg P g^{-1} dry weight [DW]) to severe P deficiency (<1,000 μg P g^{-1} DW; Supplemental Table S1). No visual symptoms of P deficiency were observed on the leaves except for a marginal anthocyanin production on the most P-deficient plants. However, typical signs of latent P deficiency were found (Fig. 1), including increased root to shoot ratio, decreased tillering, reduced biomass, and only slightly decreased chlorophyll concentrations (Supplemental Table S2). Carotenoid concentrations were not significantly affected, and element analysis of the leaves showed that the plants suffered from no additional

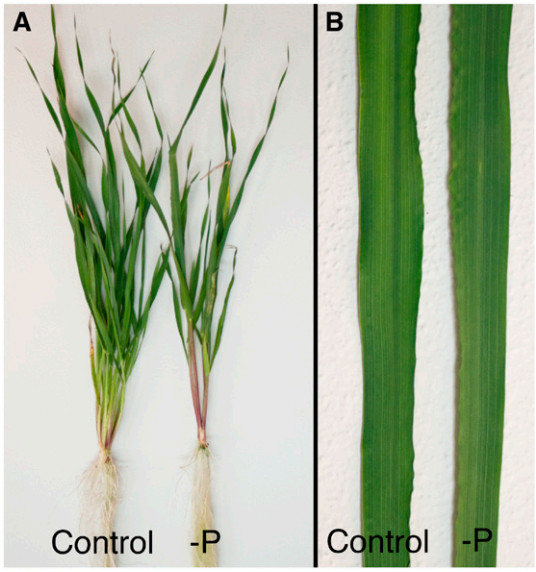

Figure 1. Control and P-deficient barley plants grown in hydroponics. A, Increased root to shoot ratio and a decrease in tillering and shoot weight are evident for the P-deficient plant compared with the healthy control plant. B, No symptoms were visible on the youngest fully developed leaves of control versus P-deficient plants, indicating latent P deficiency.

nutrient deficiencies other than P (Supplemental Table S1). The visual signs of P deficiency would therefore only be noticed if plants could be directly compared to control plants of similar age, thus making in situ visual diagnosis practically impossible.

OJIP transients measured on the youngest fully developed leaf (YFDL) of hydroponically grown control plants with sufficient P status showed normal polyphasic transients with four distinct steps (Fig. 2). By contrast, P-deficient plants showed deviating OJIP curves in which the I step measured at 20 to 50 ms straightened and almost completely vanished, whereas the shapes of the O, J, and P steps appeared unaffected (Fig. 2).

The appearance of the I step depended dynamically on the P status of the barley plants. Thus, the I step was observable in 21-d-old plants (Fig. 3) that had attained a moderate P deficiency (1,200 μg P g^{-1} DW in YFDL; Supplemental Table S1; Reuter et al., 1997). However, as the plants gradually became more severely P deficient, the I step completely disappeared (28-d-old plants with 900 μg P g^{-1} DW in YFDL; Fig. 3). Resupply of P to the nutrient solution to the 28-d-old plants caused the I step to reappear to control levels within 2 d (30-d-old plants; Fig. 3). A faster recovery was observed when incubating a P-deficient leaf in a P solution. Here, the I step started to reemerge within 30 min, and a full reappearance was seen within 120 min (Supplemental Fig. S1).

Consistent with P being a phloem-mobile nutrient (Hawkesford et al., 2012), the effect of P deficiency was observed in the second YFDL prior to being observed in the YFDL (Supplemental Fig. S2A).

Joly et al. (2010) reported that applying a far-red light pulse to specifically reduce PSI prior to measuring the OJIP transient of dark-adapted leaves resulted in a fading of the I step. Subjecting both P-deficient and healthy control barley leaves to a 60-s far-red light pulse prior to measuring the OJIP transients (Supplemental Fig. S2B) led to a complete elimination of the observed difference between healthy and P-deficient plants when measured without prior reduction of PSI (Fig. 2).

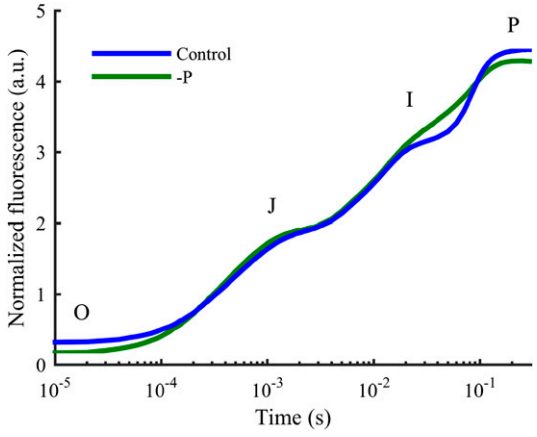

Figure 2. Typical OJIP transients from a healthy control (blue) and a P-deficient (green) barley plant. The I step is seen to have straightened and disappeared in the OJIP transient from the P-deficient plant, whereas the shape of the O, J, and P are unaffected. The OJIP transients, measured in arbitrary units (a.u.), have been normalized by F_0 and subjected to the curve correction as described in "Materials and Methods."

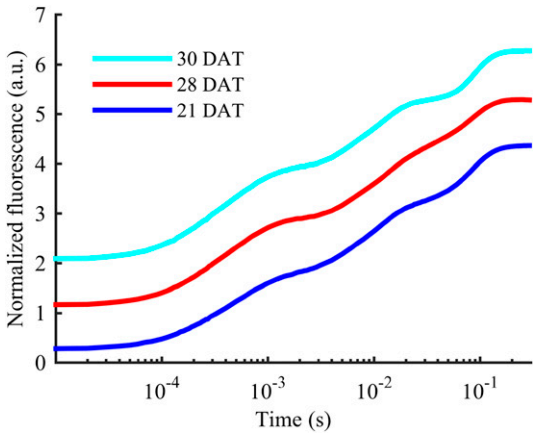

Figure 3. OJIP transients for the YFDL of a barley plant growing at the lowest level of P supply. Each transient has been offset by 1 arbitrary unit (a.u.) to improve legibility. It is seen that the I step gradually straightens and disappears as plants become increasingly P deficient from 21 DAT (1,200 μg P g^{-1} DW) to 28 DAT (900 μg P g^{-1} DW). Two days after plants were resupplied with P at 28 DAT, the I step had reappeared to a control-like state.

Similarly, the barley mutant *Viridis-zb*^{63} has been shown to be almost completely devoid of PSI activity (Nielsen et al., 1996). While the OJIP transients show very low maximum fluorescence, the preprocessing allows for comparing the shape of the OJIP transients measured from the *Viridis-zb*^{63} mutant to OJIP transients from a control plant. Doing so, it is clearly observed that the I step is completely absent in the OJIP transient from the *Viridis-zb*^{63} mutant (Supplemental Fig. S2C).

Predicting the Bioactive P Concentration in Barley Leaves

The chlorophyll *a* fluorescence measurements on the YFDL of barley plants grown in both hydroponics and in soil resulted in a data set with 701 OJIP transients. All OJIP transients were normalized by F_0 and subjected to a correction, allowing differences in the overall slope and offset of the transients to be normalized across all experiments. Thereafter, the transients were differentiated, scaled and, smoothed to augment the observed straightening of the I step (Supplemental Fig. S3). The resulting preprocessed OJIP transients were used for development and testing of a partial least-squares regression (PLS) model predicting the P concentration in each leaf.

The development and calibration of the PLS model was based on the first 300 ms (i.e. up to the P step) of OJIP transients measured on hydroponically grown

barley plants in experiment 1 (see "Materials and Methods"). During the development of the model, it became evident that the OJIP transients appeared not to respond to high P concentrations. Including leaves with concentrations up to 3,600 μg P g^{-1} DW, a total of 159 OJIP transients provided the basis for development of a PLS model with a low prediction error (Fig. 4A) that successfully predicted concentrations up to the sufficiency range for barley at 3,000 μg P g^{-1} DW (Reuter et al., 1997).

For validation of the PLS model, 291 OJIP transients measured in three completely independent experiments including soil- and hydroponically cultivated barley plants (experiments 2, 3, and 4) were taken into account. Of these transients, 131 fell within the 0 to 3,600 μg P g^{-1} DW concentration range. To minimize overfitting, a very rigorous cross-validation procedure was used in which one-half of the calibration transients were excluded in each cross-validation step. Three principal components were found to be optimal for predicting the leaf P concentrations (Fig. 4A). This limited number of principal components taken together with very comparable root-mean-squared error of calibration (369) and root mean squared error of prediction (379) for the validation transients (Fig. 4A) revealed that overfitting was not a problem. Furthermore, the regression vector for the PLS model (Supplemental Fig. S4) showed that the predictions were dependent on the straightening of the I step, thus providing evidence that the PLS model reflected the initial observations of the straightening of the I step when plants become P deficient.

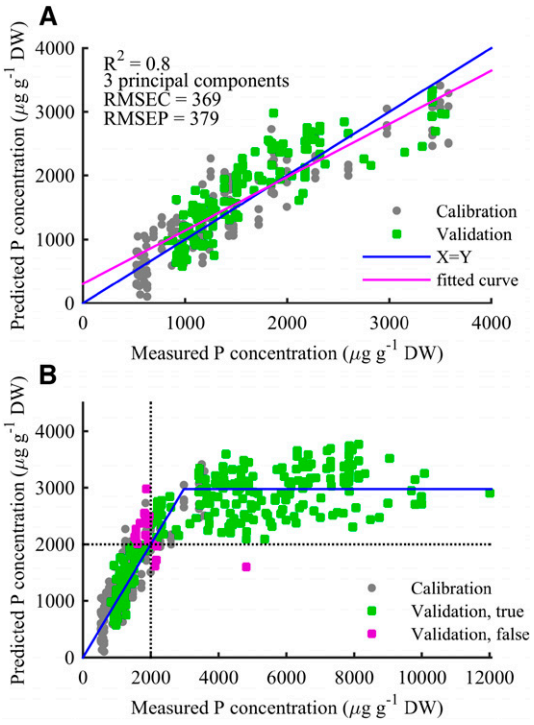

Figure 4. Predicted versus measured barley leaf P concentrations based on a PLS model with three principal components. A, PLS prediction in the calibration range. Gray circles indicate calibration samples, and red circles indicate validation samples. The blue curve indicates the optimal $Y = X$ line, and the red curve represents best linear fit to data (R^2 = 0.8). The root-mean-squared error for the 159 calibration samples (root-mean-squared error of calibration [RMSEC] = 369) is seen to be very equivalent to the root-mean-squared error for the 131 independent test samples (root-mean-squared error of prediction [RMSEP] = 379). Together with the low number of principal components used, this shows that the model is not a result of overfitting. B, Predicted versus measured P concentrations for all 448 OJIP transients. The blue curve represents the optimal fit of a $Y = X$ line intersecting a constant line at 2,975 μg g^{-1} DW. The two dotted lines indicate 2,000 μg g^{-1} DW, and coloring indicates whether the PLS model predicts samples correctly according to this threshold. Two hundred sixty-nine of 291 leaves (92%) from the test set were correctly classified as above or below the 2,000 μg g^{-1} DW threshold, and the misclassified leaves position close to the threshold except for one measurement.

The developed model was thereafter used to predict leaf P concentrations for the calibration data set as well as for all 289 OJIP transients in the validation data set with P concentration up to more than 10,000 μg P g^{-1} DW. Plotting the predicted versus the measured P concentrations clearly showed that the model was able to accurately predict leaf P concentrations at deficient levels, while leaves with a higher P concentration were predicted to an apparently constant value (Fig. 4B). Using a least-squares method to fit the intersect between a line representing an accurate PLS prediction ($Y = X$) and a constant prediction (Y = constant) gave a cutoff value of 2,975 μg g^{-1} DW (blue curve in Fig. 4B).

Field trials suggest that a leaf P concentration below 2,000 μg g^{-1} DW in the YFDL of 30-d-old barley plants leads to grain yield loss (Supplemental Table S3). For comparison, no yield losses were observed when the leaf P concentration of the YFDL was 2,300 μg g^{-1} DW or higher. Setting a threshold at 2,000 μg g^{-1} DW, the generated PLS model was able to correctly classify 269 out of the 291 leaves (92%) in the validation set as either P deficient or sufficient (Fig. 4B). For the 22 misclassified leaves, the actual measured P concentration was very close to the 2,000 μg P g^{-1} DW threshold, except for one leaf measured to have a concentration above 4,000 μg g^{-1} DW but predicted below 2,000 μg g^{-1} DW. This leaf was from a soil-grown plant resupplied with P.

Specificity of the P Effect

To test whether the observed effect of P deficiency was specific to P among other essential plant nutrients, a principal component analysis (PCA) model was developed for OJIP transients collected in this experiment as well as in previous experiments (Hebbern et al., 2009; Husted et al., 2009; Schmidt et al., 2013). In these studies, OJIP transients were measured on barley and tomato plants exposed to Ca, Cu, Fe, K, Mg, Mn, N, P, S, or Zn deficiency, along with healthy control plants.

Consistent with the previously reported strong effect of Mn on chlorophyll *a* fluorescence transients (Husted et al., 2009), Mn-deficient leaves dominated the variance described by the PCA and were clearly distinguishable from other deficiencies in the first principal component explaining 73% of the variance (Supplemental Fig. S5). However, observing principal components 2 and 5 (Fig. 5), it was evident that the P-deficient leaves from all experiments (including both barley and tomato leaves) clustered in the first quadrant of this subspace and that this group could be separated from all other nutrient deficiencies. Furthermore, S-deficient leaves clustered in the third quadrant of the same principal component subspace, and Cu-deficient leaves clustered on the border between the first and fourth quadrant. Considering the strong effect of Mn deficiency on OJIP transients, it was not surprising that the explained variance of the principal component subspace showing a P clustering only constituted 12.6% of the total variation (Fig. 5).

Looking at the loadings for principal components 2 and 5 (Supplemental Fig. S6), it was evident that principal component's 2 and 5 depended greatly on the I step of the OJIP transient, further corroborating the connection between a fading I step and P deficiency. Comparing the OJIP transients from P-deficient plants to those from S- and Cu-deficient plants (Supplemental Fig. S7), it was clear that while the I step was affected, the change of shape was distinctly different compared with the P-deficient plants. From the unprocessed fluorescence transients (Supplemental Fig. S7), S deficiency seemed to cause a more pronounced I step compared with even the control curves. For Cu-deficient plants, it appeared that the P step in particular was lowered, leading to a cutoff rather than a step at the I step.

DISCUSSION

P Deficiency and the Fading I Step

A straightening and gradual fading of the I step of the polyphasic OJIP transients was observed when plants were exposed to increasing severity of P deficiency (Fig. 3). P has several key functions in plants, including a structural role in nucleic acids, biomembranes, and NADPH and ATP syntheses as well as in regulation of metabolism via phosphorylation (Hawkesford et al., 2012). Despite these essential roles, P deficiency has not previously been shown to have a direct impact on the photosynthetic electron transport chain (Engels et al., 2012; Hawkesford et al., 2012) and hence on the OJIP transients, apart from experiments with severely P-deficient plants, which causes chlorophyll loss and decreased maximum quantum yield of PSII due to photooxidative stress (Hernández and Munné-Bosch, 2015).

Changes in the I-P phase of OJIP transients indicate an effect on the photosynthetic electron transport chain beyond cytochrome b_6f (Pospísil and Dau, 2002; Schansker et al., 2005; Joly and Carpentier, 2007; Antal and Rubin, 2008; Laisk et al., 2009). Furthermore, the observed elimination of the differences between OJIP transients from control and P-deficient plants with prior reduction of PSI using far-red light (Supplemental Fig. S2B; Joly et al., 2010) indicates a linkage between P deficiency and the electron transport in the vicinity of PSI (Schansker et al., 2005). This linkage is also supported by the observation that the I step is completely absent in OJIP transients from *Viridis-zb*^{63} mutant (Supplemental Fig. S2C). The sigmoidal rise of the I-P phase may accordingly result from a dynamic bottleneck involving a transient inactivation of ferredoxin-NADP$^+$ reductase by carbon metabolites of the Calvin

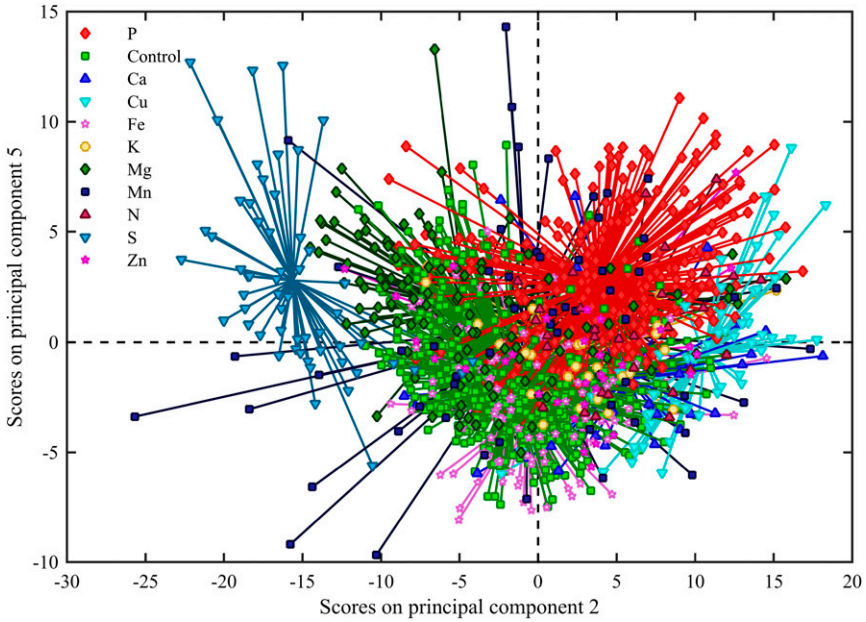

Figure 5. Score plot showing principal components 2 and 5 derived from a PCA analysis of OJIP transients from both barley and tomato plants with different nutrient deficiencies. Principal components 2 and 5 explained 10.0% and 2.6% of the variance, respectively. P-deficient samples clustered in the first quadrant. S-deficient samples are clustered in the second quadrant, and Cu-deficient samples are also seen to cluster on the border between the fourth and first quadrant.

cycle during dark adaptation (Schansker et al., 2005). Several enzymes of the Calvin cycle are known to be regulated by stromal orthophosphate and triose-P levels, ultimately influencing ATP and NADPH consumption (Rychter and Rao, 2009). Thus, it is conceivable that the I-P phase represents this final and slowest rate-limiting step of the photosynthetic electron transport chain and that it is modulated by the rate of NADPH consumption in the Calvin cycle. However, the primary mechanisms of P deficiency and the identity of the underlying processes reflected in the OJIP transient, particularly the I step, remain largely speculative (Schansker et al., 2011, 2014; Stirbet and Govindjee, 2012).

In this study, it was demonstrated that the effect of P deficiency was reversible when resupplying plants with P (Fig. 3; Supplemental Fig. S1), indicating that the disturbances to key processes were apparent and detectable before the photosynthetic apparatus had been permanently damaged. The unsupervised clustering of P-deficient tomato and barley plants in the PCA score plots (Fig. 5) highlights that a unique fingerprint of P deficiency was identified and that it was pertinent for both mono- and dicotyledonous species. The observed effect of P therefore appears to be associated with the electron transport of photosynthesis and thus constitutes a strong analytical tool to monitor the P status of higher plants in general.

Among the elements tested (N, P, K, Mg, Ca, S, Mn, Fe, Cu, and Zn), specific clustering was also observed for the elements S, Fe, Mg, Mn, and Cu (Fig. 5; Supplemental Fig. S5). S in particular shows a surprisingly clear grouping in the PCA plot (Fig. 5), which suggests that a unique fingerprint can also been identified for S deficiency in plants. Only a few studies have hitherto investigated the relationship between S deficiency and the resulting changes in chlorophyll *a* fluorescence transients. Antal et al. (2006) observed a striking suppression of the JIP phase in OJIP transients from S-deficient *Chlamydomonas reinhardtii*, similar to our observations (Supplemental Fig. S7). This was speculated to be caused by perturbations of both the donor and acceptor side of PSII, but no experimental evidence could be provided. In the classical work of Terry (1976), it was shown that the photosynthetic apparatus is a primary target of S deficiency and that it reduces photosynthesis via decreased levels of Rubisco activity, light-harvesting chlorophyll antenna, and ATP generation by photophosphorylation. Moreover, it has been shown that S deficiency affects electron transport between PSII and PSI and that it strongly impairs the ability of PSI to photoreduce $NADP^+$ (Lunde et al., 2008). This is presumably done via a lower abundance of prominent electron carrier proteins such as cytochrome b_6f and ferredoxin as well as the PSI supercomplex. All these proteins share the common feature that they contain one or more Fe-S cofactors (Chitnis, 2001). This area, and the clustering likewise observed for Fe, Mg, Mn, and Cu (Fig. 5; Supplemental Fig. S5), represents obvious areas for future research.

Predicting the Bioactive P Concentration Using OJIP Transients and Chemometrics

To test the ability of OJIP transients to predict the P concentrations in leaf tissue, a PLS model was successfully generated. As indicated by the fitted cutoff value (Fig. 4b), it was possible to predict the P concentration of the barley YFDL up to the reported sufficiency level around 3,000 $\mu g\ g^{-1}$ DW (Reuter et al., 1997). Furthermore, for 92% of all validation samples, it was possible to correctly classify whether leaves contained above or below 2,000 $\mu g\ P\ g^{-1}$ DW. Field experiments suggest that this concentration constitutes a threshold for 30-d-old plants, leading to yield losses if no additional P fertilizer is added (Supplemental Table S3). The successful classification therefore shows that the technique is sufficiently sensitive to detect latent P deficiency before the yield potential is negatively affected, which allows for timely foliar P fertilization to correct the deficiency. Plants well supplied with P are known to store up to 85% to 95% of total P as a nonmetabolic pool in the cell vacuoles (Lauer et al., 1989). This explains the inability to predict P concentrations above the 3,000 $\mu g\ g^{-1}$ DW sufficiency level of the YFDL of barley plants. When P sufficiency has been reached, the metabolic processes reflected in the OJIP transients are saturated so that provision of additional P will have no effect. The OJIP transients are therefore effectively probing the bioactive P concentration in leaves.

The observed discrepancy between the fitted cutoff value around 3,000 $\mu g\ P\ g^{-1}$ DW and the inclusion of leaves with up to 3,600 $\mu g\ g^{-1}$ DW in the development of the PLS model reflects that there were a limited number of leaves with a concentration close to 3,000 $\mu g\ P\ g^{-1}$ DW in the calibration data set. It was therefore necessary to include leaves up to 3,600 $\mu g\ g^{-1}$ DW to get a sufficient representation of healthy P-sufficient leaves in the model.

Due to the simplicity of performing chlorophyll *a* fluorescence measurements, the observed specificity and successful prediction model demonstrate that OJIP transients can be used as a valuable probe to determine the bioactive P concentration of crops. This dynamic fluorescence analysis constitutes a strong tool for establishing unique site-specific P fertilization strategies based on timely measurements of the actual P status of the crop, thereby ensuring optimal yields while avoiding excessive use of natural P resources. Additionally, our results indicate that similar detection of other nutrient deficiencies might also be possible; future studies are thus needed to show whether multielement characterization of latent nutrient deficiency using chlorophyll *a* fluorescence is possible.

MATERIALS AND METHODS

Cultivation of Plants

Barley (*Hordeum vulgare* 'Quench') plants were cultivated in hydroponics (experiments 1, 2, and 4) or in soil (experiment 3) with different levels of P

availability. Barley seeds were pregerminated for 8 d (hydroponic experiments) or 4 d (soil experiment) in vermiculite in a greenhouse with minimum day/night temperatures of 18°C/15°C and a 16-h-day/8-h-night light regime. All nutrient solutions were prepared in Milli-Q water (Milli-Q Element). Control plants were supplied with a nutrient solution containing 200 μM KH_2PO_4, 200 μM K_2SO_4, 300 μM $MgSO_4 \cdot 7\,H_2O$, 100 μM NaCl, 300 μM $Mg(NO_3)_2 \cdot 6\,H_2O$, 900 μM $Ca(NO_3)_2 \cdot 4\,H_2O$, 600 μM KNO_3, 50 μM Fe(III)-EDTA-Na, 2 μM H_3BO_3, 0.8 μM $Na_2MoO_4 \cdot 2\,H_2O$, 0.7 μM $ZnCl_2$, 1.0 μM $MnCl_2 \cdot 4\,H_2O$, and 0.8 μM $CuSO_4 \cdot 5\,H_2O$. Different levels of P deficiency were induced, with hydroponically grown plants being supplied with combinations of the treatments P100, P50, P25, and P10 containing 89, 45, 22, and 9 μM KH_2PO_4, respectively, to induce different P concentrations in the plants. A detailed description of the cultivation of the plants is included in Supplemental Text S1.

Measurements

Chlorophyll a Fluorescence

Chlorophyll *a* fluorescence transients (OJIP transients) were measured using a Handy PEA chlorophyll fluorometer (Hansatech Instruments). The midsection of the YFDL was dark adapted for at least 20 min before measuring, and a short, nonactinic light flash was used to adjust the gain of the detector. The actual measurement was conducted by illuminating the leaf with continuous actinic light at a saturating intensity (>3,000 μmol m^{-2} s^{-1}) for 10 s from three red LEDs, optically filtered to a maximum wavelength of 690 nm. The fluorescence transients were recorded using a PIN photodiode and a filter to ensure only wavelengths greater than 700 nm were recorded.

In experiment 1, measurements were performed on the YFDL 21 and 28 days after transplantation (DAT), giving 320 OJIP transients. In experiment 2, measurements were performed on the YFDL 21, 23, 28, and 30 DAT, giving 64 OJIP transients. Measurements on the second YFDL were also performed. In experiment 3, measurements were performed on the YFDL 3, 4, 5, and 6 weeks after transplanting, giving 120 OJIP transients. In experiment 4, measurements were performed on the YFDL 21, 28, and 31 DAT, giving a total of 200 OJIP transients. Measurements on the *Viridis-zb*^{63} mutant were performed 9 d after sowing (after 16 h of dark adaption); eight OJIP transients were obtained. To specifically reduce PSI, barley YFDLs from control and P25 treatments were harvested 21 DAT and illuminated for 60 s (720 nm; 30 μmol m^{-2} s^{-1}) using a PAM-101 fluorometer connected with a near-infrared dual-E emitter and a dual-DR detector (Walz). Quickly hereafter, the clip was attached, and the OJIP transient was recorded as described above. The measurements were performed under green light.

To inoculate leaves with P, barley YFDLs from a P10 treatment were harvested 28 DAT and cut into three midleaf sections of 5 cm. The sections were immersed in 1 M KH_2PO_4 containing 0.2 mL L^{-1} Tween 20 for 30, 60, or 120 min (four leaf sections in each treatment). After inoculation, the leaves were wiped, a clip was attached and dark adapted for 20 min in a zip bag, and the OJIP transient was recorded. As a control, leaves from the same P10 treatment were immersed in Milli-Q water with 0.2 mL L^{-1} Tween.

Chlorophyll, Carotenoid, and Anthocyanin Concentration

Concentrations of chlorophylls and carotenoids were determined in leaf material from the midsection of the YFDL as described by Lichtenthaler and Wellburn (1983) using methanol and determined by UV-Vis spectroscopy (Genesys 10S, Thermo Scientific). Determination of anthocyanin concentrations was performed according to the method described by Ticconi et al. (2001) using the same leaf material as described above. An EON microplate spectrophotometer (BioTek Instruments) was used to measure the absorbance at 535 and 650 nm and calculate the anthocyanin concentration.

Element Analysis

Leaf concentrations of P, Fe, Mg, Mn, Zn, K, S, and Ca were determined using inductively coupled plasma-optical emission spectroscopy (Optima 5300DV, PerkinElmer) following the procedure described in Laursen et al. (2011) and Hansen et al. (2009). YFDLs from experiment 1 were freeze dried and grounded in zirconium-coated jars containing a zirconium-coated ball in a ball mill (MM301, Retsch), whereas YFDLs from experiments 2, 3, and 4 and the field experiment were oven dried at 50°C until completely dry. Data quality was evaluated by including at least five samples of digested, certified reference material (NIST 1515, apple [*Malus* spp.] leaf, National Institute of Standards and Technology) in each analytical run. Data were processed using the WinLab32 software (version 3.1.0.0107; PerkinElmer).

Chemometric Analysis

Data were analyzed by the chemometric methods PCA (Martens and Næs, 1989) and PLS (Wold et al., 2001), carried out using Matlab R2015a (Mathworks) and PLS_Toolbox 7.9 (Eigenvector Research).

Preprocessing

As the observed effect of P deficiency affected the second and higher order components, all OJIP transients were normalized by F_0 and subtracted by 1 to have origin at 0. The resulting fluorescence transients were then first-order corrected to minimize lower order variations by a method similar to multiplicative scatter correction and standard normal variate preprocessing (Geladi et al., 1985; Helland et al., 1995). This adjusted the overall offset and slope of all transients, yet did not affect the second and higher order components of the curves. All OJIP transients were subsequently differentiated, scaled, and smoothed using a Savitzky-Golay filter (Savitzky and Golay, 1964). For more details, see Supplemental Text S1.

For the PCA, the full data set used for the analysis was additionally mean centered to emphasize variations from the mean OJIP transient over the included data set of transients from both this experiment and previous experiments (Hebbern et al., 2009; Husted et al., 2009; Schmidt et al., 2013). Leaves with a P concentration above 3,000 μg g^{-1} DW were marked as healthy control leaves, and leaves with a P concentration below 2,000 μg g^{-1} DW were marked as P deficient. Leaves between these boundaries (2,000–3,000 μg g^{-1} DW) were not included in this particular analysis.

Outlier Detection

Data outliers were detected based on interpretations of score plots of the principal components included in the PCA and PLS analyses as well as plots showing the Q residuals and Hotelling T^2 (Hotelling, 1931) parameters for each transient.

One hundred fifty-nine OJIP transients from 38 independent growth units were included in the calibration data set. Two hundred ninety-one of 382 OJIP transients were included in the validation data set. In the PCA, 35 OJIP transients were removed as outliers, leaving a data set of 1,228 OJIP transients. For more details, see Supplemental Text S1.

Supplemental Data

The following supplemental materials are available.

Supplemental Figure S1. Temporal evolution of P-resupplied leaf.

Supplemental Figure S2. Effects on OJIP transients.

Supplemental Figure S3. Fluorescence rate of change.

Supplemental Figure S4. PLS regression vector.

Supplemental Figure S5. PCA scores plots.

Supplemental Figure S6. PCA loadings.

Supplemental Figure S7. OJIP transients from Cu-, S-, and P-deficient plants.

Supplemental Table S1. Inductively Coupled Plasma-Mass Spectrometry elemental analysis results.

Supplemental Table S2. Harvest data.

Supplemental Table S3. Field trial data.

Supplemental Text S1. Additional information.

ACKNOWLEDGMENTS

We thank Lena Byrgesen and Thomas H. Hansen for assistance with the multielement inductively coupled plasma-optical emission spectroscopy analyses.

Received June 2, 2015; accepted July 7, 2015; published July 10, 2015.

LITERATURE CITED

Antal T, Rubin A (2008) In vivo analysis of chlorophyll *a* fluorescence induction. Photosynth Res **96:** 217–226

Antal TK, Volgusheva AA, Kukarskih GP, Bulychev AA, Krendeleva TE, Rubin AB (2006) Effects of sulfur limitation on photosystem II

functioning in *Chlamydomonas reinhardtii* as probed by chlorophyll *a* fluorescence. Physiol Plant **128:** 360–367

Chitnis PR (2001) PHOTOSYSTEM I: function and physiology. Annu Rev Plant Physiol Plant Mol Biol **52:** 593–626

Cordell D, Drangert JO, White S (2009) The story of phosphorus: global food security and food for thought. Glob Environ Change **19:** 292–305

Edixhoven JD, Gupta J, Savenije HHG (2013) Recent revisions of phosphate rock reserves and resources: reassuring or misleading? An in-depth literature review of global estimates of phosphate rock reserves and resources. Earth System Dynamics Discussions **4:** 1005–1034

Elser J, Bennett E (2011) Phosphorus cycle: a broken biogeochemical cycle. Nature **478:** 29–31

Engels C, Kirkby E, White P (2012) Mineral nutrition, yield and source: sink relationships. *In* P Marschner, ed, Marschner's Mineral Nutrition of Higher Plants. Elsevier, London, pp 85–133

Foley JA, Ramankutty N, Brauman KA, Cassidy ES, Gerber JS, Johnston M, Mueller ND, O'Connell C, Ray DK, West PC, et al (2011) Solutions for a cultivated planet. Nature **478:** 337–342

Food and Agriculture Organization of the United Nations (2009) Feeding the world, eradicating hunger. http://www.fao.org/fileadmin/templates/wsfs/Summit/WSFS_Issues_papers/WSFS_Background_paper_Feeding_the_world.pdf (June 24, 2015)

Geladi P, MacDougall D, Martens H (1985) Linearization and scatter-correction for near-infrared reflectance spectra of meat. Appl Spectrosc **39:** 491–500

Gilbert N (2009) Environment: the disappearing nutrient. Nature **461:** 716–718

Godfray HCJ, Beddington JR, Crute IR, Haddad L, Lawrence D, Muir JF, Pretty J, Robinson S, Thomas SM, Toulmin C (2010) Food security: the challenge of feeding 9 billion people. Science **327:** 812–818

Govindjee (2004) Chlorophyll *a* fluorescence: a bit of basics and history. *In* GC Papageorgiou, Govindjee, eds, Chlorophyll *a* Fluorescence: A Signature of Photosynthesis. Springer, Dordrecht, The Netherlands, pp 1–41

Hansen TH, Laursen KH, Persson DP, Pedas P, Husted S, Schjoerring JK (2009) Micro-scaled high-throughput digestion of plant tissue samples for multi-elemental analysis. Plant Methods **5:** 12

Harbinson J, Rosenqvist E (2003) An introduction to chlorophyll fluorescence. *In* Practical Applications of Chlorophyll Fluorescence in Plant Biology. Springer, Boston, MA, pp 1–29

Hawkesford M, Horst W, Kichey T, Lambers H, Schjoerring J, Møller IS, White P (2012) Functions of macronutrients. *In* P Marschner, ed, Marschner's Mineral Nutrition of Higher Plants. Elsevier, London, pp 135–189

Hebbern CA, Laursen KH, Ladegaard AH, Schmidt SB, Pedas P, Bruhn D, Schjoerring JK, Wulfsohn D, Husted S (2009) Latent manganese deficiency increases transpiration in barley (*Hordeum vulgare*). Physiol Plant **135:** 307–316

Helland IS, Næs T, Isaksson T (1995) Related versions of the multiplicative scatter correction method for preprocessing spectroscopic data. Chemom Intell Lab Syst **29:** 233–241

Hernández I, Munné-Bosch S (2015) Linking phosphorus availability with photo-oxidative stress in plants. J Exp Bot **66:** 2889–2900

Hotelling H (1931) The generalization of student's ratio. Ann Math Stat **2:** 360–378

Husted S, Laursen KH, Hebbern CA, Schmidt SB, Pedas P, Haldrup A, Jensen PE (2009) Manganese deficiency leads to genotype-specific changes in fluorescence induction kinetics and state transitions. Plant Physiol **150:** 825–833

Jiang HX, Tang N, Zheng JG, Li Y, Chen LS (2009) Phosphorus alleviates aluminum-induced inhibition of growth and photosynthesis in *Citrus grandis* seedlings. Physiol Plant **137:** 298–311

Joly D, Carpentier R (2007) The oxidation/reduction kinetics of the plastoquinone pool controls the appearance of the I-peak in the O–J–I–P chlorophyll fluorescence rise: effects of various electron acceptors. J Photochem Photobiol B **88:** 43–50

Joly D, Jemâa E, Carpentier R (2010) Redox state of the photosynthetic electron transport chain in wild-type and mutant leaves of *Arabidopsis thaliana*: impact on photosystem II fluorescence. J Photochem Photobiol B **98:** 180–187

Kastori R, Plesnicar M, Arsenijevic-Maksimovic I, Petrovic N, Pankovic D, Sakac Z (2000) Photosynthesis, chlorophyll fluorescence, and water relations in young sugar beet plants as affected by sulfur supply. J Plant Nutr **23:** 1037–1049

Kautsky H, Hirsch A (1931) Neue versuche zur kohlensäureassimilation. Naturwissenschaften **19:** 964

Laisk A, Eichelmann H, Oja V (2009) Leaf C3 photosynthesis in silico: integrated carbon/nitrogen metabolism. *In* A Laisk, L Nedbal, Govindjee, eds, Photosynthesis in Silico. Springer Netherlands, Dordrecht, The Netherlands, pp 295–322

Larbi A, Abadía A, Morales F, Abadía J (2004) Fe resupply to Fe-deficient sugar beet plants leads to rapid changes in the violaxanthin cycle and other photosynthetic characteristics without significant de novo chlorophyll synthesis. Photosynth Res **79:** 59–69

Lauer MJ, Blevins DG, Sierzputowska-Gracz H (1989) P-nuclear magnetic resonance determination of phosphate compartmentation in leaves of reproductive soybeans (*Glycine max* L.) as affected by phosphate nutrition. Plant Physiol **89:** 1331–1336

Laursen KH, Schjoerring JK, Olesen JE, Askegaard M, Halekoh U, Husted S (2011) Multielemental fingerprinting as a tool for authentication of organic wheat, barley, faba bean, and potato. J Agric Food Chem **59:** 4385–4396

Lichtenthaler HK, Wellburn AR (1983) Determinations of total carotenoids and chlorophylls *b* of leaf extracts in different solvents. Biochem Soc Trans **11:** 591–592

Lin ZH, Chen LS, Chen RB, Zhang FZ, Jiang HX, Tang N (2009) CO_2 assimilation, ribulose-1,5-bisphosphate carboxylase/oxygenase, carbohydrates and photosynthetic electron transport probed by the JIP-test, of tea leaves in response to phosphorus supply. BMC Plant Biol **9:** 43

Lunde C, Zygadlo A, Simonsen HT, Nielsen PL, Blennow A, Haldrup A (2008) Sulfur starvation in rice: the effect on photosynthesis, carbohydrate metabolism, and oxidative stress protective pathways. Physiol Plant **134:** 508–521

MacDonald GK, Bennett EM, Potter PA, Ramankutty N (2011) Agronomic phosphorus imbalances across the world's croplands. Proc Natl Acad Sci USA **108:** 3086–3091

Mallick N, Mohn FH (2003) Use of chlorophyll fluorescence in metal-stress research: a case study with the green microalga *Scenedesmus*. Ecotoxicol Environ Saf **55:** 64–69

Martens H, Næs T (1989) Multivariate Calibration. John Wiley & Sons Chichester, UK

McAlister ED, Myers J (1940) The Time Course Of Photosynthesis and Fluorescence Observed Simultaneously. Smithsonian Miscellaneous Collections, Washington, DC

Nielsen VS, Scheller HV, Møller BL (1996) The photosystem I mutant viridis-zb63 of barley (*Hordeum vulgare*) contains low amounts of active but unstable photosystem I. Physiol Plant **98:** 637–644

Obersteiner M, Peñuelas J, Ciais P, van der Velde M, Janssens IA (2013) The phosphorus trilemma. Nat Geosci **6:** 897–898

Pospísil P, Dau H (2002) Valinomycin sensitivity proves that light-induced thylakoid voltages result in millisecond phase of chlorophyll fluorescence transients. Biochim Biophys Acta **1554:** 94–100

Reuter DJ, Robinson JB, Dutkiewicz C (1997) Plant Analysis: An Interpretation Manual, Ed 2. CSIRO Publishing, Collingwood, Australia

Ripley BS, Redfern SP, Dames JF (2004) Quantification of the photosynthetic performance of phosphorus-deficient *Sorghum* by means of chlorophyll-*a* fluorescence kinetics. S Afr J Sci **100:** 615–618

Rychter A, Rao I (2009) Role of phosphorus in photosynthetic carbon metabolism. *In* M Pessarakli, ed, Handbook of Photosynthesis, Ed 2. Taylor & Francis, Boca Raton, FL, pp 123–148

Savitzky A, Golay MJE (1964) Smoothing and differentiation of data by simplified least squares procedures. Anal Chem **36:** 1627–1639

Schansker G, Tóth SZ, Holzwarth AR, Garab G (2014) Chlorophyll *a* fluorescence: beyond the limits of the Q_A model. Photosynth Res **120:** 43–58

Schansker G, Tóth SZ, Kovács L, Holzwarth AR, Garab G (2011) Evidence for a fluorescence yield change driven by a light-induced conformational change within photosystem II during the fast chlorophyll *a* fluorescence rise. Biochim Biophys Acta **1807:** 1032–1043

Schansker G, Tóth SZ, Strasser RJ (2005) Methylviologen and dibromothymoquinone treatments of pea leaves reveal the role of photosystem I in the Chl *a* fluorescence rise OJIP. Biochim Biophys Acta **1706:** 250–261

Schmidt SB, Pedas P, Laursen KH, Schjoerring JK (2013) Latent manganese deficiency in barley can be diagnosed and remediated on the basis of chlorophyll *a* fluorescence measurements. Plant Soil **372:** 417–429

Schröder JJ, Smit AL, Cordell D, Rosemarin A (2011) Improved phosphorus use efficiency in agriculture: a key requirement for its sustainable use. Chemosphere **84:** 822–831

Stirbet A, Govindjee (2011) On the relation between the Kautsky effect (chlorophyll *a* fluorescence induction) and photosystem II: basics and applications of the OJIP fluorescence transient. J Photochem Photobiol B **104:** 236–257

Stirbet A, Govindjee (2012) Chlorophyll *a* fluorescence induction: a personal perspective of the thermal phase, the J-I-P rise. Photosynth Res **113:** 15–61

Tang N, Li Y, Chen LS (2012) Magnesium deficiency-induced impairment of photosynthesis in leaves of fruiting *Citrus reticulata* trees accompanied by up-regulation of antioxidant metabolism to avoid photo-oxidative damage. J Plant Nutr Soil Sci **175:** 784–793

Terry N (1976) Effects of sulfur on the photosynthesis of intact leaves and isolated chloroplasts of sugar beets. Plant Physiol **57:** 477–479

Ticconi CA, Delatorre CA, Abel S (2001) Attenuation of phosphate starvation responses by phosphite in Arabidopsis. Plant Physiol **127:** 963–972

Veneklaas EJ, Lambers H, Bragg J, Finnegan PM, Lovelock CE, Plaxton WC, Price CA, Scheible WR, Shane MW, White PJ, et al (2012) Opportunities for improving phosphorus-use efficiency in crop plants. New Phytol **195:** 306–320

Weng XY, Xu HX, Yang Y, Peng HH (2008) Water-water cycle involved in dissipation of excess photon energy in phosphorus deficient rice leaves. Biol Plant **52:** 307–313

Wold S, Sjöström M, Eriksson L (2001) PLS-regression: a basic tool of chemometrics. Chemom Intell Lab Syst **58:** 109–130

Yang GH, Yang LT, Jiang HX, Li Y, Wang P, Chen LS (2012) Physiological impacts of magnesium-deficiency in *Citrus* seedlings: photosynthesis, antioxidant system and carbohydrates. Trees (Berl) **26:** 1237–1250